International Journal of Applied Pharmaceutics

ISSN- 0975-7058 Vol 16, Issue 5, 2024

Original Article

HESPERETIN DERIVATIVES AS PPAR γ AGONIST: A PHARMACOPHORE APPROACH

RAMANATHAN MUTHIAH[1*], VIJAYALAKSHMI CHINNIAH[1], MAIDA ENGELS S. E.[2]

[1*]Department of Pharmacology, PSG College of Pharmacy, Peelamedu, Coimbatore-641004, India. [2]Department of Pharmaceutical Chemistry, PSG College of Pharmacy, Peelamedu, Coimbatore-641004, India

*Corresponding author: Ramanathan Muthiah; *Email: muthiah.in@gmail.com

Received: 23 May 2024, Revised and Accepted: 09 Jul 2024

ABSTRACT

Objective: The study focuses on enhancing the pharmacological activity of hesperetin, a bioflavonoid, to develop novel derivatives with improved efficacy and reduced side effects compared to existing Thiazolidinediones (TZDs) as PPAR γ agonist.

Methods: The Methodology involves various computational approaches, including pharmacophore modelling, molecular docking, Molecular Mechanics with Generalised Born and Surface Area Solvation (MMGBSA), and molecular dynamics simulations. Pharmacophore modelling identifies essential binding features validated by Quantitative Structure-Activity Relationship (QSAR) models. Database screening and docking confirm lead compounds' binding affinity, with MMGBSA aiding lead optimization. Toxicological assessment ensures drug likeness and bioavailability. Molecular dynamics simulations explore protein-ligand complex stability and dynamics, revealing insights into their interactions.

Results: The results indicate MOL-297 exhibits improved properties over hesperetin, including ADME properties, solubility, blood-brain barrier permeability, docking score, and binding energy. Molecular dynamics simulations confirm Mol-297-PPAR γ complex stability, with favourable ligand-amino acid interactions.

Conclusion: The developed new molecule MOL 297, is a novel Peroxisome Proliferator-Activated Receptor (PPAR) gamma agonists with enhanced pharmacological properties, warranting further experimental validation and drug development.

Keywords: Hesperetin derivatives, PPAR γ agonists, Thiazolidinediones (TZDs), Molecular docking, MOL 297

DOI: https://dx.doi.org/10.22159/ijap.2024v16i5.51538 Journal homepage: https://innovareacademics.in/journals/index.php/ijap

INTRODUCTION

PPAR gamma agonists, also referred to as peroxisome proliferator-activated receptor gamma agonists, are a class of drugs that stimulate the PPAR gamma receptor. This receptor, a nuclear receptor, plays a vital role in controlling glucose and lipid metabolism, as well as inflammation regulation [1].

Peroxisome Proliferator-Activated Receptor gamma (PPAR γ) has two isoforms: PPAR γ1 and PPAR γ2 [2]. These isoforms are generated through alternative splicing of the PPAR γ gene and have distinct functions and distributions in tissues. PPAR γ1 is the primary isoform present in various tissues like adipose tissue [3], skeletal muscle [4], liver, and vascular endothelium. It is crucial in regulating adipogenesis, lipid metabolism, insulin sensitivity, and inflammation. PPAR γ1 also plays a role in mediating the metabolic effects of Thiazolidinedione (TZD) drugs, which are synthetic PPAR γ agonists. Conversely, PPAR γ2 is mainly expressed in adipose tissue, particularly in mature adipocytes [3, 5]. It is essential for adipocyte differentiation and maintaining adipocyte function, especially in regulating genes related to lipid metabolism and adipokine secretion. PPAR γ2 is the primary target for the antidiabetic effects of TZD drugs [6].

Although both isoforms have similar functions and regulatory mechanisms, they differ in tissue expression patterns and physiological roles. Understanding the unique functions and regulation of PPAR γ1 and PPAR γ2 is essential for developing targeted therapies for metabolic disorders such as type 2 diabetes and obesity [7].

The most well-known PPAR γ agonists are TZD or glitazones, which include drugs like pioglitazone and rosiglitazone. These medications function by activating PPAR γ receptors in adipose tissue, skeletal muscle, and the liver, resulting in improved glucose utilization and decreased hepatic glucose output [8]. Despite the known side effects of PPAR γ agonists, such as weight gain, fluid retention, and an increased risk of heart failure, research into these drugs continues. Efforts are being made to develop new medications that can effectively control glycemic levels while minimizing these adverse effects [9]. One example of a PPAR γ agonist that faced market withdrawal due to concerns about cardiovascular events is rosiglitazone [10, 11].

Hesperetin, a bioflavonoid and, more specifically a flavanone, is found in high concentrations in the peel of citrus fruits compared to the fleshy part. Flavanones are the most prevalent subclass of flavonoids in Citrus species [12] and are characterized by the absence of a double bond between carbons 2 and 3 in the flavonoid skeleton as shown in fig. 1. Grapefruit contains naringenin, oranges contain hesperetin, and lemons contain eriodictyol as their primary aglycones. Flavanones can also naturally occur in these forms.

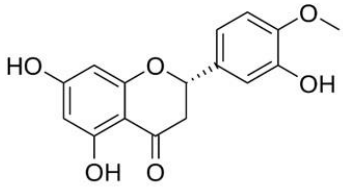

Fig. 1: Two dimensional structure of hesperetin

Flavanones are glycosylated with disaccharides, specifically the neohesperidose group at position 7. This glycosylation is believed to impact the antioxidant activity of flavanones by potentially interfering with the interaction between the methoxyl group [13, 14] at position 4 of the sugar molecule [15]. The earlier studies have shown interaction of hesperetin glucuronides with PPAR γ protein and exhibited agonistic activity [16]. In comparison to PPARγ agonist TZD, the aminoacid interaction was shown to be different with hesperetin. Therefore it can be presumed that due to difference in binding interaction, the pharmacological activity might also differ. Hence in the present study modified hesperetin molecule was

developed to have similar binding characters and interaction like PPAR γ agonist TZD.

MATERIALS AND METHODS

Protein preparation

The Research Collaboratory for Structural Bioinformatics Protein Data Bank (RCSB PDB) was used to download the crystal structures of PPAR (PDB ID: 5Y2T), with resolution of 1.70 Å (fig. 2). Based on the protein structure's lesser resolution, the chosen structures were picked. [17]The PPAR-lobeglitazone complex consists of 454 water molecules, two lobeglitazone molecules, and two chains (chains A and chain B). The PPAR Ligand Binding Domain (LBD) is composed of 13 helices, including the C-terminal (AF2-H12), and is arranged in a multi-layered sandwich structure with alpha helices and β-stranded sheets.

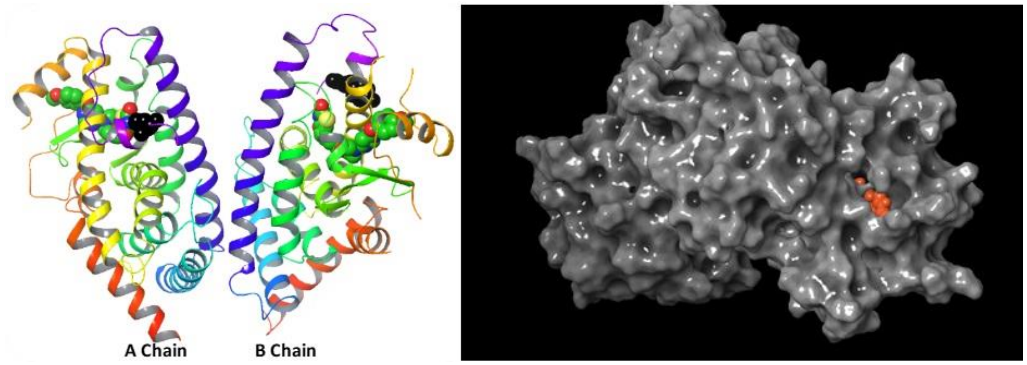

Fig. 2: Structure of PPARγ with LBD

Protein refinement was carried out utilizing the protein preparation wizard of Schrodinger. The protein preparation process involved four essential steps: import, pre-process, review, and modify [18]. Upon importing a structure, the initial step in the process involves addressing the primary structural concerns. These concerns include assigning bonds and bond orders, adding hydrogens, filling in any missing loops or side chains, capping uncapped termini, adjusting bonds and formal charges for metals, and rectifying any mislabelled elements. Additionally, it is possible to remove water molecules that are located beyond a specific distance from the het groups and align the protein structure with another protein structure. This pre-processing stage is crucial for subsequent structure preparation actions, such as generating het states, assigning H-bonds, and performing minimization.

Receptor grid generation

In this step, the molecule coupled to the protein structure was used to define the internal and external receptor grid boxes, which were 10 10 10 and 20 20, respectively. Optimized Potentials for Liquid Simulations (OPLS5) was the force field energy employed during the creation of the receptor grid. Penalties were reduced by allowing a Vander wall radius scaling of 1.0 and a partial charge cutoff value of 0.25 for non-polar atoms [19, 20].

Ligand preparation

A set of 148 hesperetin derivatives [21–25] were collected from the literature based on the anti-inflammatory, apoptosis and neuroprotective effect. In this work, the biological activities were all expressed as $pIC50=-\log_{10}IC50$.

LigPrep generates potential stereoisomers, tautomers, and states at physiological pH or any other user-defined pH in addition to converting the 2D chemical structure into a 3D energy-minimized molecular structure. The conformers from the ligand preparation process were used to create a database using the Create Phase Database panel in the PHASE v3.8 module of the Schrodinger maestro [26].

Pharmacophore generation

In this study, the phase module of the Schrodinger suite (Schrodinger, LLC, New York) was used for pharmacophore generation. Here, a crystal structure (PDB code: 5Y2T) of PPARγ complexed with lobeglitazone was used in this approach. The phase module provides a set of 5 pharmacophore features such as Hydrogen bond Acceptor (A), Donor (D), Aromatic ring (R), and Hydrophobic (H) [27, 28].

Finding common pharmacophores and scoring hypothesis

Active and inactive thresholds of $pIC_{50,}$ 7.000 and 4.500, respectively were applied to the dataset to yield 19 active and 16 inactive molecules, which were used for pharmacophore generation and subsequent scoring.

Model validation

All hypotheses produced in the last step were then used to build three-dimensional QSAR models. The dataset was randomly divided into a training and test set (standard 3:1 ratio) by using the "Automated Random Selection" option present in the PHASE program. Care was taken to ensure that the most inactive and active molecules were included in the training set. The activity data of the training set was evaluated by the generated QSAR models to assess the quality of the pharmacophore hypothesis [29, 30].

Database screening

The best pharmacophore model was used as a search query to retrieve molecules with novel and desired chemical features from the commercially available database [30].

Molecular docking

Drug candidates from database screening were docked using GLIDE V7.7 from the Schrodinger suite (Schrodinger, LLC, New York) to identify e-pharmacophore-matched compounds. The docking process was performed in flexible mode with extra-precision (XP) settings to analyze the highest-ranking hits and establish scoring restrictions [31]. Torsional constraints were maintained at their default values. The selection of top compounds was based on their docking score, G-score, and binding interactions, utilizing GLIDE v7.7 [32].

MMGBSA

The PRIME MM/GBSA program utilized the equation below to forecast the binding free energy (G bind) of the Ligand docked complexes with VSGB as an implicit solvent model:

$$\Delta G\ bind = \Delta Emm+\Delta Gsolv+\Delta Gsa$$

The binding free energy (ΔG bind) is equal to the sum of the changes in the electrostatic interaction energy (ΔEmm), solvation free energy (ΔGsolv), and surface area energy (ΔGsa) [33].

Toxicology prediction using QikProp v5.4

The QikProp tool in Maestro v11.9 was utilized to analyze the initial Absorption, Distribution, Metabolism and Excretion (ADME)

properties of the chosen ligands. Schrödinger QikProp v5.4 was employed for the prediction of ADME properties. Post structure-based virtual screening; the ligands underwent further filtration based on ADME properties using the QikProp tool. QikProp offers a comprehensive set of key characteristics to comprehend Absorption, Distribution, Metabolism, Excretion, and toxicity (ADME/tox). These descriptors encompass forecasted blood-brain barrier partition coefficient (logBB), anticipated aqueous solubility (QPlogS), hydrophilic group (FISA), Solvent Accessible Surface Area (SASA) and elucidates the bioavailability of orally active medications etc [34].

Molecular dynamics

The stability of complex formation in a biologically inspired setting was evaluated by subjecting complexes to a molecular dynamics simulation using DESMOND V5.2. The TIP3P model was utilized, and all protein-ligand complexes were solvated in orthorhombic boxes. Counterions such as Na+ and Cl-ions were added to neutralize the system at a salt concentration of 0.15M. The OPLS_2005 force field was then applied to loosen the system. To gain a comprehensive understanding of the dynamics of the small molecule during its interaction, the equilibrated system was simulated for 100 ns using the NPT ensemble class after multiple energy minimization stages [31].

The resulting MD trajectory was analyzed using various metrics, including PL-RMSD, RMSF, SSE distribution of residual index, % Protein-ligand interactions, and ligand torsion profile. The stability of complex formation was assessed and compared to co-crystal complexes.

RESULTS

Pharmacophore modeling research yielded multiple four- and five-point common pharmacophore hypothesis (fig. 3). The four-featured hypothesis were excluded from the scoring analysis because they did not match the active compounds' common locations. A common pharmacophore hypothesis acquired with ADHRR-1 was utilized to generate 3D QSAR models. Focusing primarily on pharmacophore models with scores in the top 1%, the most predictive QSAR model was found to be connected with the five-point hypothesis ADHRR-1.

3D QSAR model and validation

The obtained QSAR model was validated by various statistical parameters, such as r2 (Squared Correlation Coefficient), Q2 (Cross Validated Correlation Coefficient), Pearson-R, SD (Standard Deviation), RMSE (Root mean Square Error), and F-value (Variance Ratio) for the selected CPH, which are shown in fig. 4. The high r2 (0.9788) and q2 (0.7825) values demonstrate the model's predictive power. The high values of R2 and variance ratio (F) for this model demonstrate its statistical robustness. Statistical significance ($P<0.05$) suggests higher levels of confidence.

This means F is significant at 95% level. The low SD and RMSE obtained in the present study indicate that the model is significant. The intersite distances and angles of the CPH with a significant QSAR model (ADHRR 1) are shown in fig. 3 and table 1. The superimposition of ADHRR 1 with the most active (fig. 4) showed that the most active compounds map very well with the pharmacophore model.

Table 1: Interbond distance and angle

Atom 1	**Atom 2**	**Atom 3**	**Angle**
A3	D9	R13	67.4
A3	D9	R14	34.5
D9	R13	R14	16.5
H12	A3	D9	83.8
H12	D9	A3	73
H12	D9	R14	38.9
H12	R14	A3	127.1
R13	A3	D9	80.4
R13	A3	H12	7.3
R13	A3	R14	38.1
R13	R14	A3	126.2
R14	A3	D9	42.3
R14	H12	R13	13.9
Site 1	**Site 2**	**Distance**	
A3	R14	2.782	
D9	A3	4.782	
D9	H12	12.083	
D9	R13	8.833	
D9	R14	3.305	
H12	A3	11.626	
H12	R13	3.579	
H12	R14	9.735	
R13	A3	8.271	
R13	R14	6.319	

The database screening of commercially available compounds resulted in 7 Hit molecule (fig. 5), which was further filtered by ADME properties tabulated in table 2 and molecular dynamic studies. Mol-297**:**2-Oxo-2-phenylethyl 4-acetamido-1-(4-methoxybenzyl)-1H-pyrazole-3-carboxylate (Molport-046-701-621) was identified as a lead molecule.

The chain A and chain B of PPAR have nearly identical conformations; the so-called "Ω-loop," which connects H2b and H3, forms a loop structure. The Ω-loop, acting as a gateway to the ligand-binding pocket, is a highly flexible region of the LBD. Chain B has a more structured Ω-loop due to the lattice interactions stabilizing the loop. The central region is predominantly composed of nonpolar residues, such as Leucine330, Leucine339, Leucine353, and Methionine 364. However, at both ends of the ligand-binding cavity, there are clusters of polar residues. The AF-2 pocket is formed by several polar residues, including Cysteine 285, Serine289, Histidine 323, Tyrosine 327, Histidine 449, and Tyrosine 473 (fig. 6). A few polar residues, such as Glutamic acid 259, Arginine 280, and Serine 342, can be found in the Ω-pocket. The majority of the Ω pocket is composed of hydrophobic residues from the sheet, including IsoLeucine249, Methionine 348, and Isoleucine341, as well as H2b (Leucine 255, Glycine258, and Isoleucine262), and H3 (Isoleucine 281) [35, 36].

Title	Stars	Survival Score	Site Score	Vector Score	Volume Score	BEDROC Score	PhaseHypoScore
imported_structures (161)							
phase_pharm_1 (720)							
ADHRR_1 (36)	☆☆☆	5.943	0.992	0.998	0.739	1.000	1.357
ADHRR_2 (36)	☆☆☆	5.940	1.000	0.974	0.742	1.000	1.356
DDHRR_1 (36)	☆☆☆	5.937	0.986	0.999	0.640	1.000	1.356
ADHRR_3 (36)	☆☆☆	5.937	1.000	0.993	0.736	1.000	1.356
ADHRR_4 (36)	☆☆☆	5.920	1.000	0.987	0.653	1.000	1.355
ADHRR_5 (36)	☆☆☆	5.912	1.000	1.000	0.749	1.000	1.355
ADHRR_6 (36)	☆☆☆	5.903	1.000	0.954	0.721	1.000	1.354
AAHRR_1 (36)	☆☆☆	5.901	1.000	0.993	0.736	1.000	1.354
ADHRR_7 (36)	☆☆☆	5.899	1.000	1.000	0.749	1.000	1.354
DDHRR_2 (36)	☆☆☆	5.916	0.969	0.997	0.645	0.998	1.353
DHRR_1 (36)	☆☆☆	5.549	1.000	1.000	0.749	1.000	1.333
DHRR_2 (36)	☆☆☆	5.531	0.993	0.998	0.742	1.000	1.332
DHRR_3 (36)	☆☆☆	5.495	0.992	0.998	0.722	1.000	1.330
AHRR_1 (36)	☆☆☆	5.490	1.000	1.000	0.749	1.000	1.329
DHRR_4 (36)	☆☆☆	5.483	0.992	0.998	0.684	1.000	1.329
DHRR_5 (36)	☆☆☆	5.471	0.990	0.998	0.701	1.000	1.328
AHRR_2 (36)	☆☆☆	5.469	1.000	1.000	0.732	1.000	1.328
AHRR_3 (36)	☆☆☆	5.469	1.000	1.000	0.753	1.000	1.328
AAHR_1 (36)	☆☆☆	5.463	1.000	1.000	0.732	1.000	1.328
ADHR_1 (36)	☆☆☆	5.462	1.000	1.000	0.732	1.000	1.328

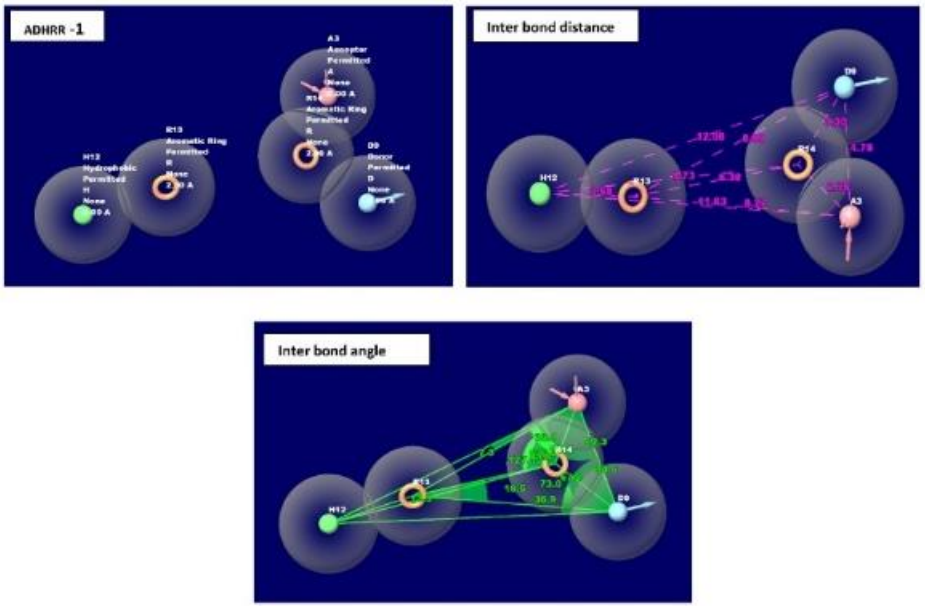

Fig. 3: Phase pharmacophore hypothesis

# Factors	SD	R^2	R^2 CV	R^2 Scramble	Stability	F	P	RMSE	Q^2	Pearson-r
1	0.9072	0.6353	0.5290	0.3085	0.981	81.9	7.27e-12	0.95	0.5955	0.7732
2	0.5050	0.8894	0.6391	0.5650	0.86	185.0	1.01e-22	0.71	0.7720	0.8824
3	0.3785	0.9399	0.6837	0.7277	0.828	234.5	1.78e-27	0.69	0.7837	0.8861
4	0.2263	0.9788	0.6912	0.8136	0.754	508.8	3.56e-36	0.72	0.7625	0.8742

** SD- Std Dev, R^2- Regression (<1), R^2 CV-cross validated, R^2 scramble -Avg value of R^2, Stability (close to 1), F- Variance Ratio (highest), P-significance level of variance ratio, RMSE-Root mean square error(<0.5), Q^2 and R-Pearson- close to 1.

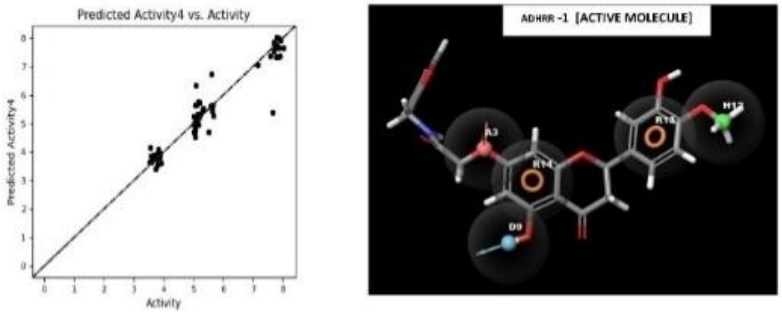

Fig. 4: Atom based QSAR

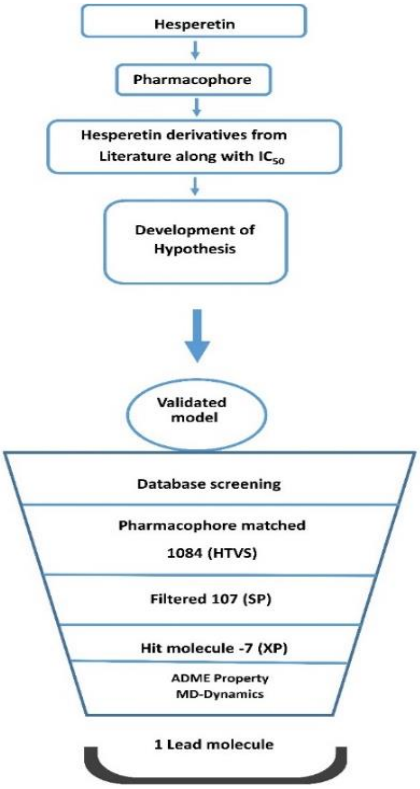

Fig. 5: Scheme of pharmacophore modelling and molecular docking-based drug discovery

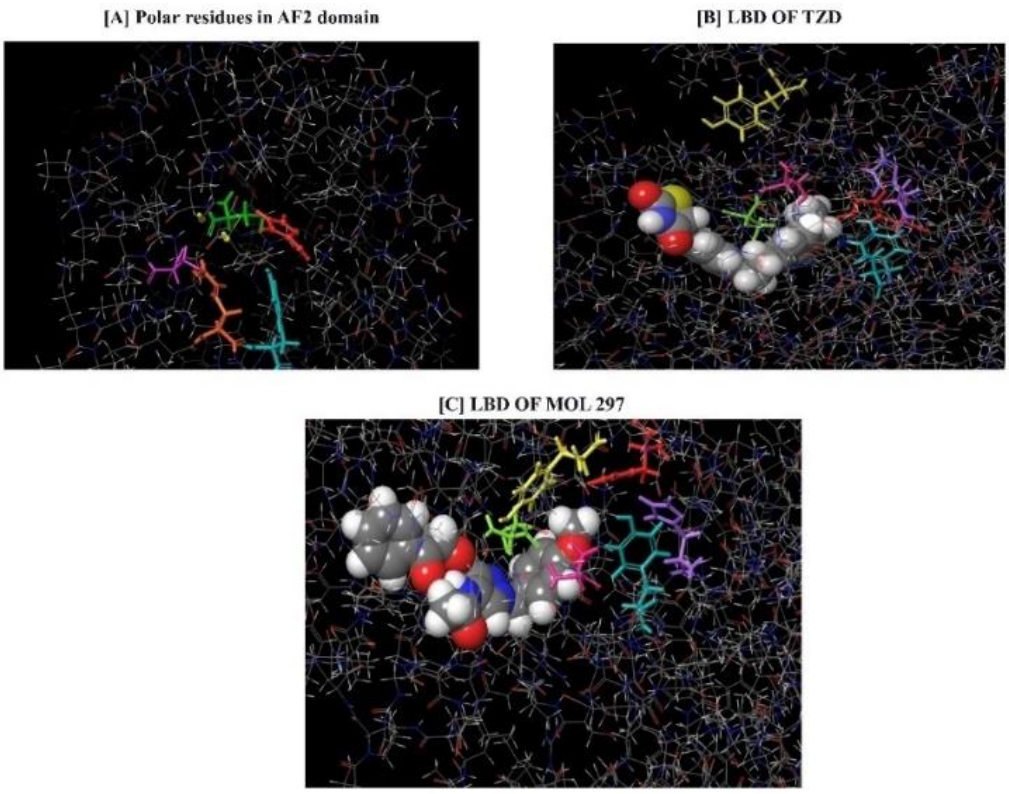

Fig. 6: LBD of PPARγ, TZD and MOL 297

The modified molecule of hesperetin, MOL 297 have shown similar interaction with amino acids like ARG 288, SER 342 and HIS 266 like the standard drug thiazolidinedione. However, the parent compound hesperetin shown interaction with aminoacid SER 342 only (fig. 7).

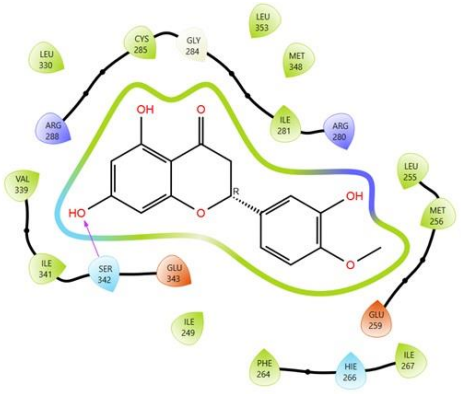

Fig. 7: Interaction of hesperetin with PPARγ

The ADME properties, aqueous solubility, ability to cross blood-brain barrier docking score and binding energy of MOL 297 was comparitively improved when compared to the parent compound hesperetin, which were tabulated in table 2.

Table 2: Toxicological properties, docking score and binding energy

Parameters	Hesperetin	Mol.297
(QPlogS) Predicted aqueous solubility, log S. S in mol dm–3	-1.764	-3.489
QlogBB	-0.9	-1.446
Percentage Human Oral absorbtion	61.586	87.665
FISA (Hydrophilic group)	158.085	267.48
SASA (Solvent assessable surface area)	398.794	666.618
Glide G Score	-7.794	-10.061
MM-GBSA Binding Energy dG bind	-60.76 Kcal/mol	-92.40 Kcal/Mol

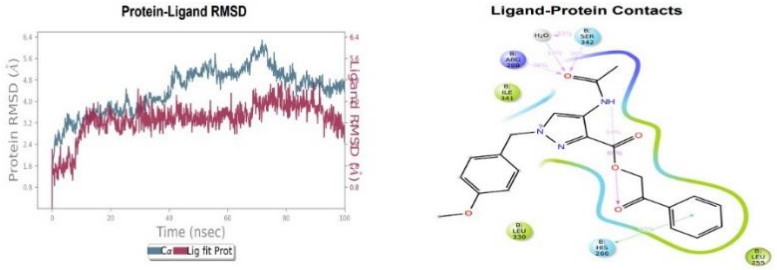

[A] Protein Ligand RMSD and Ligand-protein contacts of MOL 297

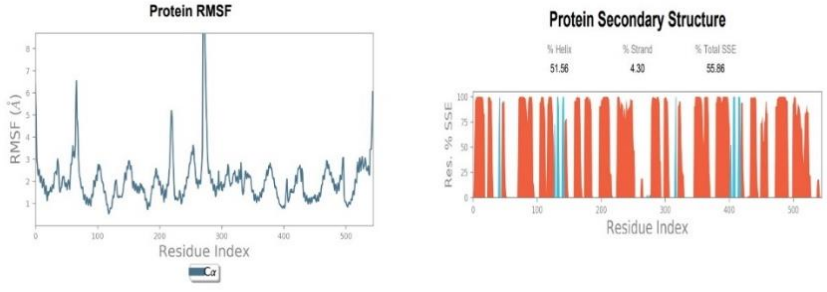

[B] Root-mean-square Fluctuations graph of mol 297

[C] Protein secondary structure of PPAR γ

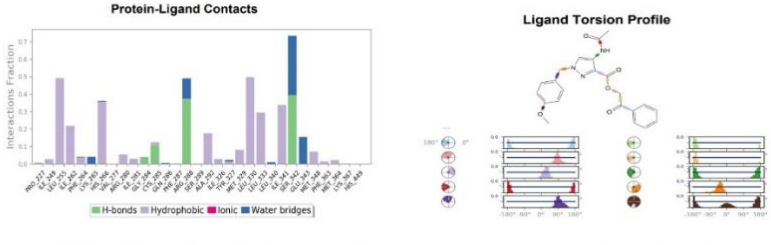

[D] Bar Diagram of protein ligand contacts

[E] 2D torsion profile of ligand

Fig. 8: Molecular dynamics-Mol 297

Molecular dynamics

The conformations produced for the top-ranked complex were analysed for 100 ns simulation, and RMSD was determined for the protein backbone, ligand RMSD, and protein side chain throughout a 100 ns simulation trajectory over a given time. Protein-ligand RMSD is used to calculate the average change in displacement of a subset of atoms for a certain frame compared to the reference frame, and LP-contacts represent a thorough report on ligand atom interactions with protein residue. The protein-ligand combination is stable (fig. 8A).

In the ligand-protein contacts the major interactions were hydrogen bond formation with ARG 288, SER-342, pi-pi cationic interaction with HIS 266.

The Root mean Square Fluctuation (RMSF) analysis within Molecular Dynamics (MD) simulations serves as a useful method for examining the flexibility and dynamic characteristics of the protein PPARγ. This analysis involves determining the average fluctuation of individual atoms within the protein structure in comparison to their mean positions throughout a 100ns timeframe. This analysis offers insights into the regions of the protein that demonstrate significant flexibility or stability (fig. 8B).

Proteins Secondary structure refers (fig. 8C) to local structural motifs within the target protein PPARγ, such as alpha helices, beta sheets, and turns. Monitoring the changes in secondary structure during the MD simulation of 100ns helps to understand the protein folding, stability, and interactions with ligands or other biomolecules. Amino acid SER 342 interaction is common in both hesperetin and MOL. 297 and the other major interactions observed in molecular dynamics are ARG 288, GLY 284, ILE 281and the remaining interactions are hydrophobic and between the water bridges (fig. 8D)

Torsional analysis

During the simulation, torsional analysis is performed to examine the dihedral angles (torsions) within the ligand molecule. Torsional angles are defined by the rotation around single bonds within the ligand structure (fig. 8E). Common torsional angles include those involving bonds between carbon atoms (C-C bonds) and sometimes between carbon and heteroatoms (e. g., C-O, C-N).

Torsional profiles provide insights into the preferred conformations of the ligand molecule and its flexibility. Peaks or multiple peaks in the torsional profile indicate preferred or energetically favorable conformations of the ligand. Changes in torsional profiles over time or in different simulation conditions can reveal dynamic behavior and conformational changes of the ligand within the protein binding site.

DISCUSSION

This study examines the potential of Hesperetin derivatives as potential Peroxisome PPARγ agonist for neuroprotection. PPARγ activation is known to suppress the production of inflammatory mediators in the brain [39, 40], offering a potential benefit for chronic neurodegenerative diseases often characterized by chronic, low-grade inflammation [2, 4]. Additionally, PPARγ activation can induce the expression of antioxidant enzymes, which combat the damaging effects of free radicals in the brain, a major contributor to neurodegeneration [3]. Studies also suggest that PPARγ agonists might promote neurogenesis and enhance neuronal survival [3], potentially slowing down or preventing neurodegeneration. Finally, PPARγ activation might contribute to maintaining the integrity of the blood-brain barrier (BBB), which protects the brain from harmful substances [3]. A compromised BBB can worsen neurodegeneration, and PPARγ agonists might offer some protective benefits [41, 42].

Previous investigations have demonstrated that hesperetin glucuronides [16] possess PPARγ agonistic activity, exhibiting distinct binding characteristics compared to TZDs. To enhance the biological activity of hesperetin and create new derivatives as PPARγ agonists, the researchers utilized pharmacophore modeling [36, 37]. This approach allowed them to identify the essential structural characteristics necessary for improving hesperetin's efficacy [43]. Among the various QSAR models [30] examined, the ADHRR-1 five-point hypothesis proved to be the most reliable, as it exhibited high r^2 (0.9788) and q^2 (0.7825) values, indicating its strong predictive capabilities [38]. Through a meticulous screening of databases, the compound MOL 297 emerged as a promising candidate. Further refinement of MOL 297 was conducted based on MMGBA (Molecular Mechanics Generalized Born Surface Area) and ADME (Absorption, Distribution, Metabolism, and Excretion) properties. Subsequent molecular dynamics simulations were performed to assess the stability of MOL 297 when interacting with the target protein PPARγ. This analysis revealed the formation of several key bonds that likely contribute to MOL 297's potential efficacy as a PPARγ agonist.

Hydrogen bonds

The analysis identified hydrogen bond formations between MOL 297 and two specific amino acids in PPARγ: Arginine (ARG) 288 and Serine (SER) 342. Hydrogen bonds are strong interactions that occur between a hydrogen atom bonded to an electronegative atom (like oxygen or nitrogen) and another electronegative atom. These interactions can play a crucial role in stabilizing the binding between MOL 297 and PPARγ.

Pi-pi cationic interaction

Additionally, the analysis revealed a pi-pi cationic interaction with Histidine (HIS) 266. Pi-pi interactions involve interactions between aromatic rings present in both MOL 297 and HIS 266. The "cationic" aspect refers to the positive charge on the HIS 266 side chain, which can further strengthen the interaction. These combined interactions likely contribute to the specific and oriented binding of MOL 297 within the PPARγ binding pocket.

CONCLUSION

The binding affinity of the hesperetin molecule with PPAR Gamma Protein was assessed through molecular docking studies. The findings revealed a clear interaction between hesperetin and the amino acid SER342 of the target protein. In comparison, the reference drug thiazolidinedione exhibited interactions with ARG 288, SER342 and HIS 266, similar to molecule 297 with the PPAR gamma protein. These results suggest that molecule 297 may possess PPAR gamma agonistic activity.

ABBREVIATIONS

QSAR-Quantitative Structure-Activity Relationship, MMGBSA-Molecular mechanics with generalised Born and surface area solvation, OPLS-Optimized Potentials for Liquid Simulations, ADME-Absorption Distribution Metabolism and Excretion, TZDs–thiazolidinediones, RCSB PDB-Research Collaboratory for Structural Bioinformatics Protein Data Bank, LBD-Ligand Binding Domain, RMSD-Root mean Square Deviation, RMSF-Root mean Square Fluctuation, SSE-Secondary Structure Analysis

ACKNOWLEDGEMENT

The work is a part of the Ph. D. Thesis of THE TAMIL NADU Dr. M. G. R. MEDICAL UNIVERSITY, Chennai.

FUNDING

No funding was received from any funding agency

AUTHORS CONTRIBUTIONS

Muthiah Ramanathan developed the concept reviewed and approved the final version. Vijayalakshmi Chinnaiah conceptualized, designed, analyzed, and wrote the manuscript. S. E. Maida Engels reviewed the QSAR part of the manuscript.

CONFLICT OF INTERESTS

No potential conflict of interest was reported by the authors.

REFERENCES

1. Bajaj M, Suraamornkul S, Hardies LJ, Glass L, Musi N, DeFronzo RA. Effects of peroxisome proliferator-activated receptor (PPAR)-α

and PPAR-γ agonists on glucose and lipid metabolism in patients with type 2 diabetes mellitus. Diabetologia. 2007;50(8):1723-31. doi: 10.1007/s00125-007-0698-9, PMID 17520238.

2. Chen Y, Jimenez AR, Medh JD. Identification and regulation of novel PPAR gamma splice variants in human THP-1 macrophages. Biochim Biophys Acta. 2006;1759(1-2):32-43. doi: 10.1016/j.bbaexp.2006.01.005, PMID 16542739.
3. Bogazzi F, Ultimieri F, Raggi F, Russo D, Manetti L, Cosci C. Abnormal expression of PPAR gamma isoforms in the subcutaneous adipose tissue of patients with cushings disease. Clin Endocrinol (Oxf). 2007;66(1):7-12. doi: 10.1111/j.1365-2265.2006.02675.x, PMID 17201795.
4. Gilde AJ, Van Bilsen M. Peroxisome proliferator-activated receptors (PPARS): regulators of gene expression in heart and skeletal muscle. Acta Physiol Scand. 2003;178(4):425-34. doi: 10.1046/j.1365-201X.2003.01161.x, PMID 12864748.
5. Vidal Puig A, Jimenez Linan M, Lowell BB, Hamann A, Hu E, Spiegelman B. Regulation of PPAR γ gene expression by nutrition and obesity in rodents. J Clin Invest. 1996;97(11):2553-61. doi: 10.1172/JCI118703, PMID 8647948.
6. Hu W, Jiang C, Kim M, Xiao Y, Richter HJ, Guan D. Isoform-specific functions of PPARγ in gene regulation and metabolism. Genes Dev. 2022;36(5-6):300-12. doi: 10.1101/gad.349232.121, PMID 35273075.
7. Wagner N, Wagner KD. The role of PPARs in disease. Cells. 2020;9(11):236. doi: 10.3390/cells9112367, PMID 33126411.
8. Thangavel N, Al Bratty M, Akhtar Javed S, Ahsan W, Alhazmi HA. Targeting peroxisome proliferator-activated receptors using thiazolidinediones: strategy for design of novel antidiabetic drugs. Int J Med Chem. 2017;2017:1069718. doi: 10.1155/2017/1069718, PMID 28656106.
9. Dumasia R, Eagle KA, Kline Rogers E, May N, Cho L, Mukherjee D. Role of PPAR-γ agonist thiazolidinediones in treatment of pre-diabetic and diabetic individuals: a cardiovascular perspective. Curr Drug Targets Cardiovasc Haematol Disord. 2005;5(5):377-86. doi: 10.2174/156800605774370362, PMID 16248830.
10. Botta M, Audano M, Sahebkar A, Sirtori CR, Mitro N, Ruscica M. PPAR agonists and metabolic syndrome: an established role. Int J Mol Sci. 2018;19(4):1197. doi: 10.3390/ijms19041197, PMID 29662003.
11. Kumar AP, PP, Kumar BR, Jeyarani V, Dhanabal SP, Justin A. Glitazones PPAR-γ and neuroprotection. Mini Rev Med Chem. 2021;21(12):1457-64. doi: 10.2174/1389557521666210304112403, PMID 33663364.
12. Lopez JG. Flavonoids in health and disease. Curr Med Chem. 2019;26(39):6972-5. doi: 10.2174/0929867326391912130954O5, PMID 31920188.
13. Banjarnahor SD, Artanti N. Antioxidant properties of flavonoids. Med J Indones. 2014;23(4):239-44. doi: 10.13181/mji.v23i4.1015.
14. Pietta PG. Flavonoids as antioxidants. J Nat Prod. 2000;63(7):1035-42. doi: 10.1021/np9904509, PMID 10924197.
15. Ullah A, Munir S, Badshah SL, Khan N, Ghani L, Poulson BG. Important flavonoids and their role as a therapeutic agent. Molecules. 2020;25(22):5243. doi: 10.3390/molecules25225243, PMID 33187049.
16. Lee MA, Tan L, Yang H, Im YG, Im YJ. Structures of PPARγ complexed with lobe-glitazone and pioglitazone reveal key determinants for the recognition of antidiabetic drugs. Sci Rep. 2017;7(1):16837. doi: 10.1038/s41598-017-17082-x, PMID 29203903.
17. Nolte RT, Wisely GB, Westin S, Cobb JE, Lambert MH, Kurokawa R. Ligand binding and co-activator assembly of the peroxisome proliferator-activated receptor-γ. Nature. 1998;395(6698):137-43. doi: 10.1038/25931, PMID 9744270.
18. Zieleniak A, Wojcik M, Wozniak LA. Structure and physiological functions of the human peroxisome proliferator-activated receptor γ. Arch Immunol Ther Exp (Warsz). 2008;56(5):331-45. doi: 10.1007/s00005-008-0037-y, PMID 18836859.
19. Schrodinger LL. Schrodinger release 2021-1: protein preparation wizard. Epic Impact Prime Schrodinger. LLC, New York; 2021.
20. Halgren TA, Murphy RB, Friesner RA, Beard HS, Frye LL, Pollard WT. Glide: a new approach for rapid accurate docking and scoring. 2. Enrichment factors in database screening. J Med Chem. 2004;47(7):1750-9. doi: 10.1021/jm030644s, PMID 15027866.
21. Friesner RA, Banks JL, Murphy RB, Halgren TA, Klicic JJ, Mainz DT. Glide: a new approach for rapid accurate docking and scoring. 1. Method and assessment of docking accuracy. J Med Chem. 2004;47(7):1739-49. doi: 10.1021/jm0306430, PMID 15027865.
22. Zheng Y, Zhang YL, Li Z, Shi W, Ji YR, Guo YH. Design and synthesis of 7-O-1,2,3-triazole hesperetin derivatives to relieve inflammation of acute liver injury in mice. Eur J Med Chem. 2021;213:113162. doi: 10.1016/j.ejmech.2021.113162, PMID 33493826.
23. Zhong G, Shen J, Chen Z, Lin Z, Long L, Wu J. Antioxidant and antitumor activities of newly synthesized hesperetin derivatives. Molecules. 2022;27(3):879. doi: 10.3390/molecules27030879, PMID 35164142.
24. Mistry B, Patel RV, Keum YS. Access to the substituted benzyl-1,2,3-triazolyl hesperetin derivatives expressing antioxidant and anticancer effects. Arab J Chem. 2017;10(2):157-66. doi: 10.1016/j.arabjc.2015.10.004.
25. Ding HW, Huang AL, Zhang YL, Li B, Huang C, Ma TT. Design synthesis and biological evaluation of hesperetin derivatives as potent anti-inflammatory agent. Fitoterapia. 2017;121:212-22. doi: 10.1016/j.fitote.2017.07.016, PMID 28774689.
26. Jung KY, Park J, Han YS, Lee YH, Shin SY, Lim Y. Synthesis and biological evaluation of hesperetin derivatives as agents inducing apoptosis. Bioorg Med Chem. 2017;25(1):397-407. doi: 10.1016/j.bmc.2016.11.006, PMID 27840137.
27. Schrodinger 2022-1. Small molecule drug discovery. Portland: Schrodinger LLC; 2022.
28. Darshit BS, Balaji B, Rani P, Ramanathan M. Identification and *in vitro* evaluation of new leads as selective and competitive glycogen synthase kinase-3β inhibitors through ligand and structure-based drug design. J Mol Graph Model. 2014;53:31-47. doi: 10.1016/j.jmgm.2014.06.013, PMID 25064440.
29. Kinarivala N, Suh JH, Botros M, Webb P, Trippier PC. Pharmacophore elucidation of phosphoiodyn a Potent and selective peroxisome proliferator-activated receptor β/δ agonists with neuroprotective activity. Bioorg Med Chem Lett. 2016;26(8):1889-93. doi: 10.1016/j.bmcl.2016.03.028, PMID 26988304.
30. Dixon SL, Smondyrev AM, Knoll EH, Rao SN, Shaw DE, Friesner RA. PHASE: a new engine for pharmacophore perception, 3D QSAR model development, and 3D database screening: 1. methodology and preliminary results. J Comput Aided Mol Des. 2006;20(10-11):647-71. doi: 10.1007/s10822-006-9087-6, PMID 17124629.
31. Faris A, Ibrahim IM, Hadni H, Elhallaoui M. High throughput virtual screening of phenylpyrimidine derivatives as selective JAK3 antagonists using computational methods. J Biomol Struct Dyn. 2024;42(14):7574-99. doi: 10.1080/07391102.2023.2240413.
32. Research DES. Desmond molecular dynamics system. New York: Schrodinger Release; 2019.
33. Zhou Z, Felts AK, Friesner RA, Levy RM. Comparative performance of several flexible docking programs and scoring functions: enrichment studies for a diverse set of pharmaceutically relevant targets. J Chem Inf Model. 2007;47(4):1599-608. doi: 10.1021/ci7000346, PMID 17585856.
34. Kumar AP, Mandal S, PP, Faizan S, Kumar BR, Dhanabal SP. Rational design molecular docking dynamic simulation synthesis PPAR-γ competitive binding and transcription analysis of novel glitazones. J Mol Struct. 2022;1265(5):133354. doi: 10.1016/j.molstruc.2022.133354.
35. Schrodinger, QikProp LL. New York, Vol. 2015; 2021.
36. Djajadisastra J, Purnama HD, Yanuar A. In silico binding interaction study of mefenamic acid and piroxicam on human albumin. Int J App Pharm. 2017;9(10):56-62. doi: 10.22159/ijap.2017.v9s1.56_62.
37. Mahfudin U, Subarnas A, Wilar G, Hermanto F. Potential activity of kaempferol as antiparkinson; molecular docking and pharmacophore modelling study. Int J App Pharm. 2023;15(3):43-8. doi: 10.22159/ijap.2023v15i3.47355.

38. Hermanto F, Syam AK, Haq FA, Rachmawan RL. Structure-based drug design method: molecular docking study and pharmacophore modelling of apigenin as an antimalarial. Int J App Pharm. 2023;15(3):272-7. doi: 10.22159/ijap.2023v15i3.47487.
39. Czech MP. Insulin action and resistance in obesity and type 2 diabetes. Nat Med. 2017 Jul 11;23(7):804-14. doi: 10.1038/nm.4350, PMID 28697184.
40. Corona JC, Duchen MR. PPARγ as a therapeutic target to rescue mitochondrial function in neurological disease. Free Radic Biol Med. 2016 Nov;100:153-63. doi: 10.1016/j.freeradbiomed.2016.06.023, PMID 27352979.
41. Hussain R, Zubair H, Pursell S, Shahab M. Neurodegenerative diseases: regenerative mechanisms and novel therapeutic approaches. Brain Sci. 2018 Sep 15;8(9):177. doi: 10.3390/brainsci8090177.
42. Pizcueta P, Vergara C, Emanuele M, Vilalta A, Rodriguez Pascau L, Martinell M. Development of PPARγ agonists for the treatment of neuroinflammatory and neurodegenerative diseases: leriglitazone as a promising candidate. Int J Mol Sci. 2023 Feb 6;24(4):3201. doi: 10.3390/ijms24043201, PMID 36834611.
43. Kaserer T, Beck KR, Akram M, Odermatt A, Schuster D. Pharmacophore models and pharmacophore-based virtual screening: concepts and applications exemplified on hydroxysteroid dehydrogenases. Molecules. 2015 Dec 19;20(12):22799-832. doi: 10.3390/molecules201219880, PMID 26703541.